ACS APPLIED MATERIALS & INTERFACES

Research Article

www.acsami.org

Reinforced Poly(Propylene Carbonate) Composite with Enhanced and Tunable Characteristics, an Alternative for Poly(lactic Acid)

Iman Manavitehrani,[†] Ali Fathi,[†] Yiwei Wang,[‡] Peter K. Maitz,[‡,§] and Fariba Dehghani*[,†]

[†]School of Chemical and Biomolecular Engineering, University of Sydney, Sydney, New South Wales 2006, Australia

[‡]Burns Research Group, ANZAC Research Institute, University of Sydney, Concord, New South Wales 2139, Australia

[§]Burns and Reconstructive Surgery Unit, Concord Repatriation General Hospital, Concord, New South Wales 2139, Australia

ABSTRACT: The acidic nature of the degradation products of polyesters often leads to unpredictable clinical complications, such as necrosis of host tissues and massive immune cell invasions. In this study, poly(propylene carbonate) (PPC) and starch composite is introduced with superior characteristics as an alternative to polyester-based polymers. The degradation products of PPC−starch composites are mainly carbon dioxide and water; hence, the associated risks to the acidic degradation of polyesters are minimized. Moreover, the compression strength of PPC-starch composites can be tuned over the range of 0.2 ± 0.03 MPa to 33.9 ± 1.51 MPa by changing the starch contents of composites to address different clinical needs. More importantly, the addition of 50 wt % starch enhances the thermal processing capacity of the composites by elevating their decomposition temperature from 245 to 276 °C. Therefore, thermal processing methods, such as extrusion and hot melt compression methods can be used to generate different shapes and structures from PPC−starch composites. We also demonstrated the cytocompatibility and biocompatibility of these composites by conducting in vitro and in vivo tests. For instance, the numbers of osteoblast cells were increased 2.5 fold after 7 days post culture. In addition, PPC composites in subcutaneous mice model resulted in mild inflammatory responses (e.g., the formation of fibrotic tissue) that were diminished from two to 4 weeks postimplantation. The long-term in vivo biodegradation of PPC composites are compared with poly(lactic acid) (PLA). The histochemical analysis revealed that after 8 weeks, the biodegradation of PLA leads to massive immune cell infusion and inflammation at the site, whereas the PPC composites are well-tolerated in vivo. All these results underline the favorable properties of PPC−starch composites as a benign biodegradable biomaterial for fabrication of biomedical implants.

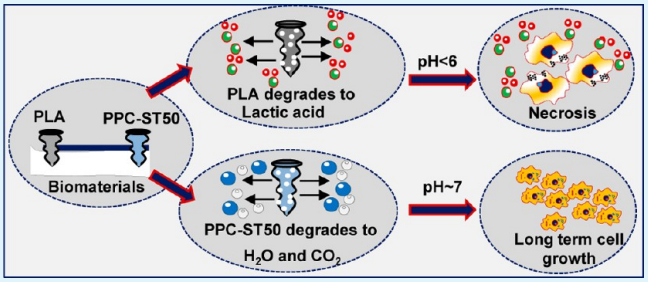

KEYWORDS: *poly(propylene carbonate), starch, composite, poly(lactic acid), biodegradable*

1. INTRODUCTION

Aliphatic polyesters are used for the fabrication of medical implants because of their biodegradation properties, processability, high mechanical strength, and favorable biocompatibility.[1,2] As an example, poly(lactic acid) (PLA) is used for the preparation of sutures, screws, and also as a scaffold for bone regeneration.[3,4] However, the secretion of lactic acid during the biodegradation of PLA resulted in the necrosis of the host cells.[5−7] Additionally, in vivo studies demonstrated that PLA interferes with the bone remodeling process and unbalances the number of osteoblast and osteoclasts during the bone remodeling.[8,9] Therefore, an alternative biodegradable polymer is desirable to eradicate all these clinical complications.

Poly(propylene carbonate) (PPC) is biodegradable aliphatic polyester, synthesized by the copolymerization of CO_2 and propylene oxide (PO).[10] It is important to note that the degradation products of PPC are CO_2 and water that are biologically benign compounds and forms a weak acid.[11] PPC is used for the formation of polymer scaffolds for tissue regeneration applications, e.g., bone and nerve regeneration.[11,12] Nanofibers of PPC were also fabricated with suitable mechanical strength, tensile and compression modulus over the range of 20−30 GPa that were used for nerve tissue regeneration.[13] However, a wider application of PPC is limited by two factors; its low glass transitional temperature and limited mechanical strength. The glass transition temperature of PPC is within the range of 25 to 45 °C that may cause unpredictable deshaping upon its in vivo application.[14] The compression strength of PPC is also within the range of 100−300 kPa, which is low for load-bearing applications.[15,16]

A variety of nano and microfillers has been used as an additive to the polymer to address their shortfall. Fillers, such as carbon nanotubes, graphene oxide, clay, and starch are used to tune the physicochemical properties of polymers.[17−20] There are unmet challenges associated with the application of carbon nanotubes and graphene for biomedical applications due to their intrinsic nondegradable properties, controversial cell proliferation behavior, and their high production cost.[21,22]

Received: July 16, 2015
Accepted: September 17, 2015
Published: September 17, 2015

DOI: 10.1021/acsami.5b06407
ACS Appl. Mater. Interfaces 2015, 7, 22421−22430

The lack of cell adhesive properties and the brittleness also limit the application of clay fillers for the load-bearing applications.[23] Starch is an abundantly available natural polysaccharide that has been widely used for a variety of biomedical applications such as drug delivery and the fabrication of composite scaffolds.[24−27] Amylose and amylopectin are the principal components of starch that degrade into glucose that is highly biocompatible.[28] Therefore, it is deemed that starch displays a great promise as a filler for enhancing the mechanical strength of PPC.

The aim of this study was to develop a biocompatible, biodegradable composite with favorable mechanical strength as an alternative to PLA-based polymers for load-bearing tissue regeneration. To this end, starch was used as a microfiller to enhance the physicochemical properties of PPC. The cytocompatibility and biocompatibility of PPC-starch composites were studied in vivo for up to 8 weeks. In addition, the degradation rate of PPC-starch composites was compared with PLA in simulated physiological conditions and their biological degradation behaviors were also examined in vivo by using mice, subcutaneous models. Following these studies, the feasibility of processing PPC-starch by various techniques such as a hot melt compression to form micropatterning and thermal extrusion was examined.

2. RESULTS AND DISCUSSION

2.1. PPC−Starch Composites. The PPC−starch composites were fabricated by melt mixing method. The melting temperature and the stirring speed were optimized to acquire the homogeneous distribution of starch particles within PPC networks. The preliminary results showed that the minimum temperature of 170 °C and the mixing speed of 300 rpm were required to ensure the uniform distribution of components. The starch composition was varied in the range of 0 wt % to 50 wt %. The distribution of starch microparticles within the composites was studied by using SEM imaging. The average particle sizes of starch granules in different composites were measured by ImageJ software using SEM images in Figure 1. For instance, the average particle size of starch in PPC-ST50 and PPC-ST40 samples were 27.81 ± 1.78 and 26.72 ± 3.27 μm, respectively that were similar to that of starch particles prior to mixing with PPC. ($p > 0.05$). These data confirmed that starch particles were not agglomerated and distributed uniformly in PPC. These results illustrated that the starch granules were not agglomerated, suggesting the homogeneous dispersion of starch within the PPC matrix. Previous studies confirmed that the presence of intermolecular interaction between the fillers and polymer matrices is essential to acquire the uniform distribution of components.[29]

ATR-FTIR analysis was used to assess the presence of intermolecular interaction between starch and PPC in the composite structures. The ATR-FTIR spectra of neat PPC in Figure 1b display two characteristic bands in the range of 1730−1750 and 1220−1240 cm^{-1} corresponding to the carbonyl group, C═O, and ether functional group, −C−O−C−, respectively.[30] Previous studies showed a shift of nearly 4 cm^{-1} to 12 cm^{-1} wavenumber for carbonyl band of PPC in the FTIR spectra as a result of molecular interactions between this polymer and starch.[31,32] We also observed a shift of carbonyl band for PPC-ST50 from 1739 to 1733 cm^{-1} wavenumber. This shift was attributed to the formation of a hydrogen bond between hydroxyl groups of starch and carbonyl groups of PPC. The SEM imaging of composite structures and the presence of

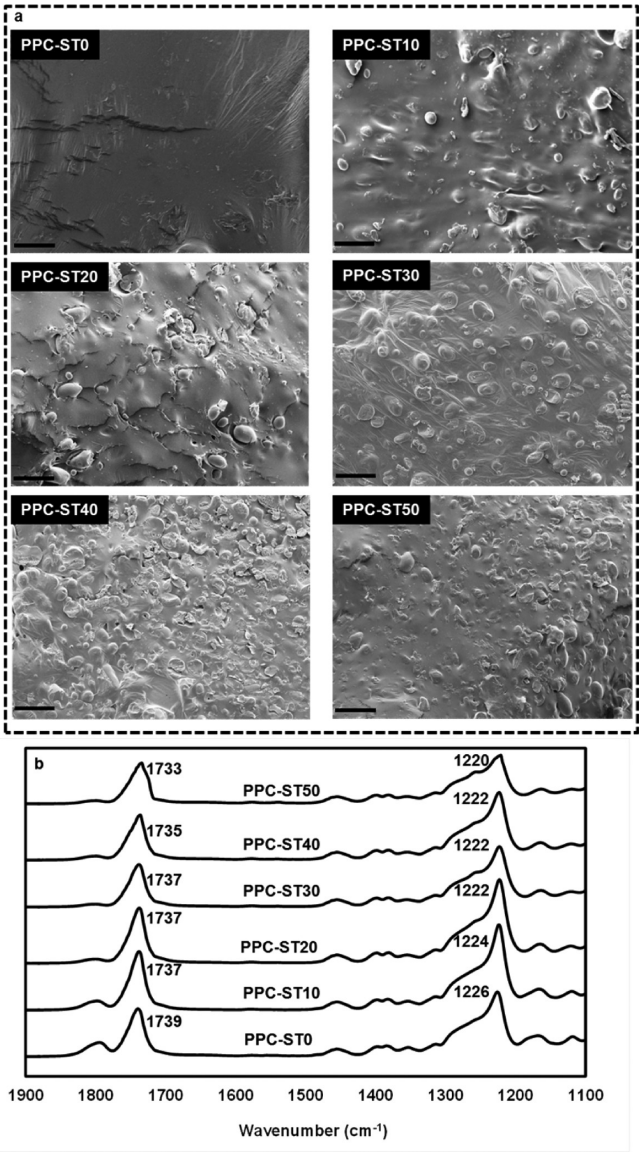

Figure 1. (a) SEM micrographs of PPC−starch composites, scale bar is 100 μm, (b) ATR FTIR spectrum of different weight ratio of PPC−starch.

intermolecular interaction between PPC and starch confirmed the formation of homogeneous PPC−starch composites.

2.2. Thermal and Mechanical Behaviors. Thermogravimetric analysis (TGA) and differential scanning calorimetry (DSC) were conducted to assess the thermal behavior of PPC-starch composites. TGA analysis in Figure 2a shows the effect of thermal heating on PPC and starch. Figure 2b showed that the untreated PPC decomposed at 150 °C due to backbiting or unzipping mechanisms of PPC.[33] This result was concluded from the presence of a strong peak in the derivative thermogravimetric analysis (DTG) of the untreated PPC. At 150 °C, the cyclic propylene carbonate, which is a byproduct of PPC synthesis, was decomposed.[34,35] The absence of peak at 150 °C in Figure 2c, d confirmed the absence of cyclic propylene carbonate in the heat-treated PPC and PPC−starch composites. This result suggested that the thermal blending of PPC and starch at 170 °C could remove toxic impurities, such as cyclic propylene carbonate, and thus can potentially enhanced the biological properties of the composites. The

DOI: 10.1021/acsami.5b06407
ACS Appl. Mater. Interfaces 2015, 7, 22421−22430

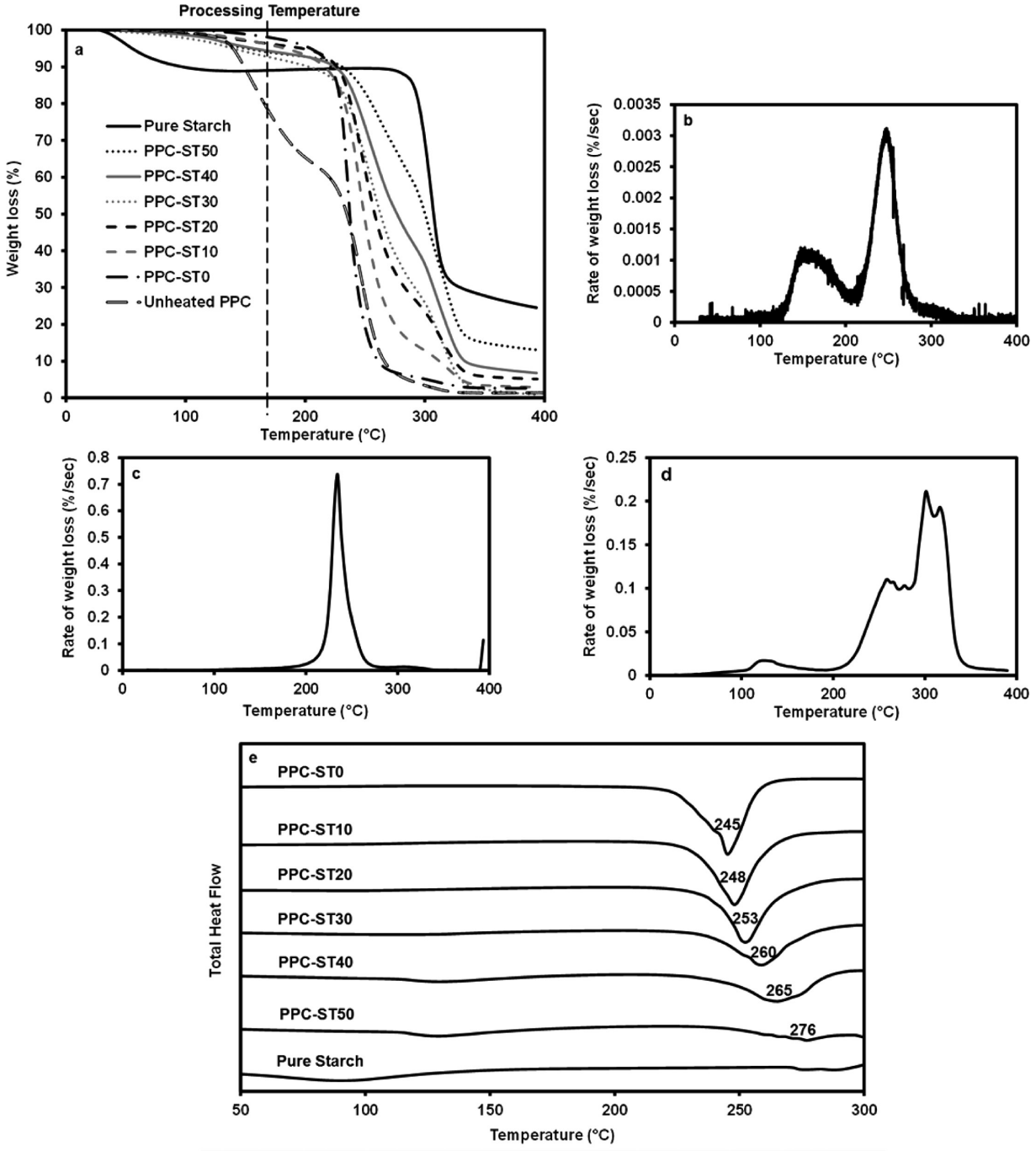

Figure 2. (a) TGA profiles of PPC, starch, and their composites, (b) DTG curves of the unheated PPC, (c) heat-treated PPC, and (d) PPC-ST50; (e) DSC results of the different PPC and starch composites.

peaks at 270 and 300 °C in the DTG profile of PPC-ST50 corresponded to the decomposition temperature of PPC and starch, respectively. These results, therefore, showed that the chemical integrity of starch and PPC were preserved at a temperature below 180 °C used for the preparation of composites. DSC analysis was also conducted to detect the characteristic temperature of different PPC-starch composites. The addition of 50 wt % starch to PPC remarkably increased the decomposition temperature from 245 to 276 °C as demonstrated in Figure 2e. These results suggested that the addition of starch promoted the thermal processing of PPC, which is a critical factor in extrusion and other thermal-based processing techniques.[36]

The effect of the addition of starch on the mechanical performance of the composites was also studied. The stress−strain curve of neat PPC and PPC-starch composites are shown in Figure 3a. The addition of starch significantly increased the compression Young's modulus of PPC as illustrated in Figure 3b. For instance, the compressive modulus of constructs was increased from 0.2 ± 0.03 MPa for neat PPC to 13.9 ± 0.57 MPa and 33.9 ± 1.51 MPa for composites with 20 and 50 wt % starch contents, respectively. A remarkable 170-fold increase of the compression strength of PPC-ST50 compared to neat PPC could extend the applications of PPC from soft tissue regeneration to hard musculoskeletal tissue repair.[37] Further increase of starch content dramatically decreased the structural

DOI: 10.1021/acsami.5b06407
ACS Appl. Mater. Interfaces 2015, 7, 22421−22430

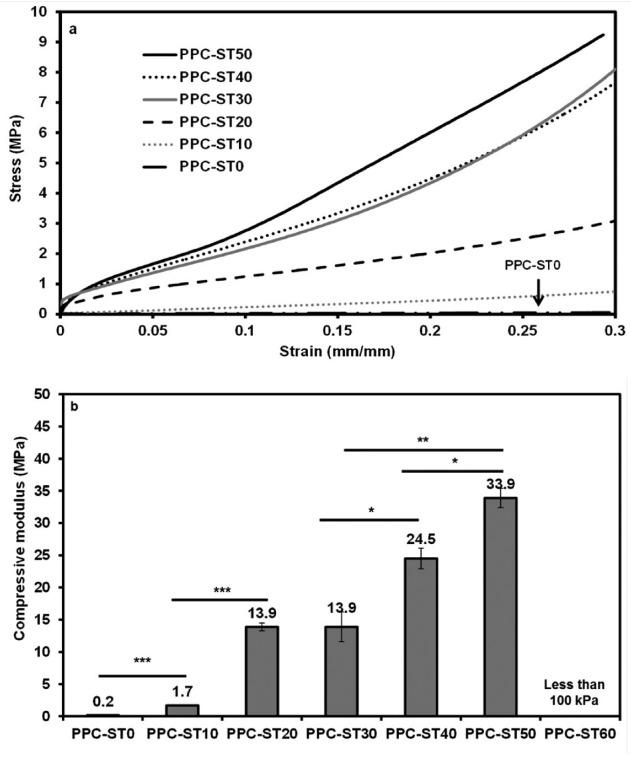

Figure 3. (a) Compressive stress−strain curves up- to 0.3 (mm/mm) strains, (b) compressive modulus of different PPC−starch composites (*p < 0.05, **p < 0.01, and ***p < 0.001).

integrity of the composites as the Young's modulus of PPC-ST60 was less than 100 kPa. Therefore, PPC-ST50 was used for further investigations and its degradation behavior was compared with pure PPC. The addition of starch particles in the ductile PPC matrix led to increasing the energy of crack propagation and material failure. Therefore, these composites acquired higher compressive modulus and were tougher.[38]

2.3. Processability of the PPC Composites. Different heat-treatment approaches are used to generate micropatterns or to form different structures for a variety of biomedical applications. Hot melt compression technique is used to produce micropatterns on the surface of polymeric structures to assess cell−cell and cell−surface interactions studies. In addition, the thermal extrusion method is commonly used for 3D printing and also for positive and negative moldings of polymers to produce structures with predefined shapes.[39−41] We examined the feasibility of using PPC-starch composites in different heat treatment processes. As depicted in Figure 4, hot melt compression and also extrusion could be used for the preparation of PPC-starch composites. Additionally micromolding technique was used to prepare microchannels, 10 μm × 100 μm on the surface of the PPC-starch composites (Figure 4b).[42] These results demonstrate that PPC-starch composites could preserve their integrity in heat treatment processes to fabricate fibers, molds, micropatterned films, and three-dimensional structures. The long-term in vitro and in vivo degradation behaviors of PPC−starch composites also need to be studied and compared with current gold standards, such as PLA.

2.4. Cell Behavior Study. The potential of using PPC composites for the load-bearing applications was investigated by culturing osteoblast cells (Saso-2) on the surface of these constructs. Cell adhesion and proliferation were assessed by using SEM imaging and MTS assay at different time points postculture. The SEM images in Figure 5a−h show the initial osteoblast attachment and spreading after 1, 6, 12, and 24 h on the surface of PPC-ST0 and PPC-ST50 samples. On both surfaces, the cells exhibited round shape after 1 h seeding whereas they attached to the surface of the samples using their pseudopods after 6 h (black arrows in Figure 5a−d). After 12 h, the migrant cells show a focal adhesion with extensive numbers of filopodia, slender cytoplasmic projections that extended beyond the leading edge, and better spreading with widely varying cell shapes (Figure 5e, f).[43,44] After 24 h, the cells on the surface of both PPC-ST0 and PPC-ST50 were mostly

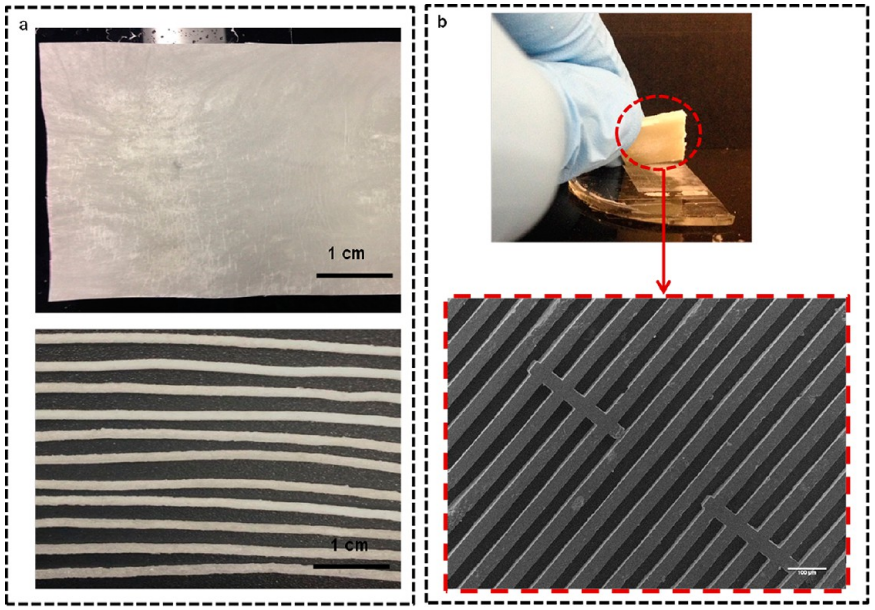

Figure 4. Processability of the PPC-ST50 composite (a) macrograph of PPC-ST50 sheet produced by hot melt compression under the following conditions: temperature, 150 °C; pressure, 7 MPa; and time, 1 h; and PPC-ST50 melted extruded fibers; (b) microchannel pattern.

DOI: 10.1021/acsami.5b06407
ACS Appl. Mater. Interfaces 2015, 7, 22421−22430

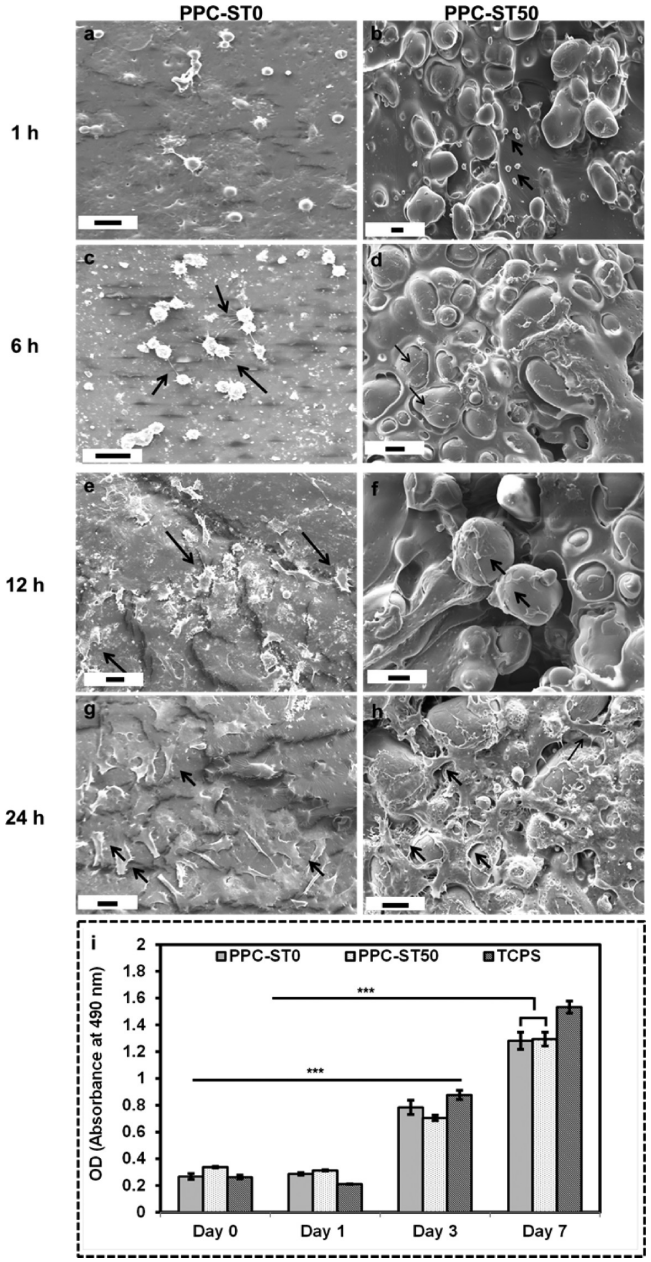

Figure 5. SEM micrographs of osteoblast cells cultured on surfaces of the PPC-ST0 and PPC-ST50 after (a, b) 1, (c, d) 6, (e, f) 12, and (g, h) 24 h, respectively; osteoblast cell proliferation results (i) from MTS assay before and after 1, 3, and 7 days ($p^{***} < 0.001$).

confluent and well covered the whole surface (Figure 5g, h). These results confirmed the cell-adhesiveness properties of PPC based constructs 24 h postculture. In addition, the long-term growth of the osteoblast cells on the surface of the composites was studied for up to 7 days to confirm the cytocompatibility of these structures in vitro.

The results in Figure 5i show that the numbers of cells, cultured on PPC-ST0 and PPC-ST50, are continuously increased by 2.5-fold ($p < 0.001$) 7 days postculture. Furthermore, at different time points, there was no significant difference among the numbers of cells on the tissue culture polystyrene (TCPS) flask (as the positive control) and the samples ($p > 0.05$). These results confirmed the cytocompatible properties of the PPC and PPC-starch composites. Favorable mechanical properties and in vitro cytocompatibility of the PPC−starch composite structures encouraged us to assess the biocompatibility of these constructs in vivo.

2.5. In Vivo Biocompatibility Study. The H&E staining of the samples demonstrated a fibrotic tissue was formed around the implants 2 weeks postoperation as a mild inflammatory response to foreign objects in vivo as shown in Figure 6a, b. However, no distinct tissue necrosis, edema, hyperemia, hemorrhaging, and muscle damages were observed during this time. The collagen-rich fibrotic capsule and neovascularization around the implant was diminished from 2 to 4 weeks postimplantation as shown in Figure 6c. No cell infiltration was noticed within these PPC-starch implants due to the nonporous structure of these constructs. In vivo subcutaneous implantation studies confirmed the favorable biological properties and biocompatibility of the PPC−starch composites. These results suggest that the PPC−starch composites may have high potential for a variety of biomedical applications.

2.6. Degradation Behavior. A cocktail of enzymatic solutions (constitutes of α-amylase and lipase) were used to simulate physiological conditions in vitro. The degradation profiles of PPC−starch, PLA, and PLGA were compared. The results in Figure 7a show that 13.35 ± 0.12% of PPC-ST50 degrades after 8 weeks. These results suggested that the degradation rate of the PPC-starch composites was comparable to that for PLA films, e.g., 8.20 ± 0.62 wt %. In addition, the SEM imaging of the composite structures in Figure 7b, c showed that after 8 weeks, starch granules were washed out from the composites as pores with diameter in the range of 20 μm are formed on the surface of the composite structures. The opaqueness of the washing media at this time point also suggested that the starch granules were removed from the composites and were suspended in the media. The degradation rate of the composites was gradually accelerated because of the formation of the pores on their surface, which increases the surface contact area between the media and the structures. It is worth to mention that the bulk degradation of PPC (a polyester-based polymer)−starch was governed by hydrolysis and enzymatic reaction.[14,45,46] In the literature, series of associated clinical complications were also reported because of the acidic degradation of PLA, PLGA, and their combination.[47−49] Therefore, we monitored the variation of pH in the washing media of PLA, PLGA, and the composite structures for up to 2 months.

Our result in Figure 7d demonstrates that the pH of the media that contained PLA and PLGA samples was dropped to 5.75 ± 0.26 and 5.94 ± 0.27, respectively, within 1 week. After 4−5 weeks, the pH of the soaking solution of PLGA samples dramatically decreased to 1.5. This sudden drop in pH was due to the bulk degradation of PLGA during this period. Within the examined period, the pH of PLA washing media approached a plateau at nearly 5.5. The reduction of pH as the result of PLA degradation can cause a severe inflammatory reaction and tissue necrosis. In particular, for bone remodeling phase, the drop of pH decreases the activity of osteoblast and thus can lead to long-term osteoporosis.[50] On the other hand, the pH of media that contained PPC−starch composites was neutral even after 2 months. This biologically benign degradation behavior of PPC-starch composites is of a great value for biomedical applications. The in vivo biomedical application of PLA is widespread from drug encapsulation to scaffolds for bone tissue engineering.[51] Therefore, it was essential to compare directly the long-term biodegradation behavior of PPC-starch composites with PLA

DOI: 10.1021/acsami.5b06407
ACS Appl. Mater. Interfaces 2015, 7, 22421−22430

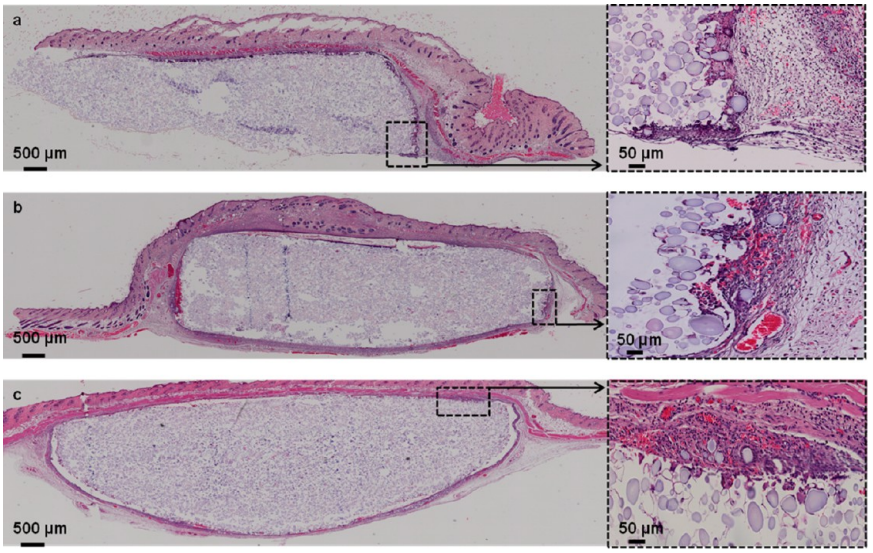

Figure 6. H&E histological photographs of skin surface treated with PPC-ST50 composites: (a) a week after surgery, (b) 2 weeks after surgery, and (c) 4 weeks after surgery. The inflammatory response increased from the first week to the second week after implantation. However, no obvious inflammation could be detected after 4 weeks postsurgery.

structures in vivo. To this end, we used mice subcutaneous implantation model and collected the samples 2 months postoperation.

The long-term biodegradation behavior of PPC−starch composites and PLA structures were compared in vivo by using six pathogen-free mice. The implants were collected two months post implantation operation. The H&E staining of the skin biopsies in Figure 8 show a very mild fibrous tissue around the PPC−starch composite structure. There was no cell invasion into the composite structures. However, a fibrotic tissue was formed around PLA constructs with massive immune cell diffusions into their structures. Previous studies also reported less mature capsules of sustained thicknesses for the PLA and high molecular weight PLGA up to 49 days.[52] All these in vitro and in vivo observations confirmed superior biodegradation behavior and biological properties of PPC−starch composites compared to PLA for tissue engineering applications.

3. CONCLUSIONS

Thermal blending method was an efficient technique to prepare a homogeneous mixture of PPC-starch. The addition of starch enhanced both thermal and mechanical properties of PPC. Our in vitro tests demonstrated that PPC-starch composite was cytocompatible as osteoblast cells adhered and proliferated on the surface of these samples for at least 7 days. Subcutaneous implantation of PPC-starch composites confirmed the biocompatibility of these constructs and their biologically benign degradation behavior. These composites were well-tolerated in vivo as the inflammation of foreign body diminished within 2−4 weeks post-implantation. All these results suggest that PPC-starch composites can be contemplated as a viable alternative to PLA to eradicate the associated clinical complications, such as host tissue necrosis and osteoporosis.

4. EXPERIMENTAL SECTION

4.1. Materials. Poly(propylene carbonate) was provided by Cardia Bioplastics Ltd. with the molecular weight (M_w) of 160 kDa and the T_g of the 37.63 °C. Soluble starch with the average size ∼25 μm (ACS reagents), Dulbecco's modified eagle medium (DMEM), phosphate buffer saline (PBS, pH 7.4), poly(D,L-lactide) IV 0.49 dL/g (average M_w 75−120 kDa), poly(D,L-lactide/glycolide) (50:50) IV 1.02 dL/g (average Mw 60−75 kDa), *Aspergillus oryzae, rhizopus oryzae* and trypsin were obtained from Sigma-Aldrich and were used without any further purification. [3-(4, 5-dimethylthiazol-2-yl)-5-(3-carboxymethoxyphenyl)- 2-(4-sulfophenyl)-2H-tetrazolium] was obtained from Promega for MTS assay. Fetal bovine serum (FBS) and antibiotic-antimycotic were purchased from Life Technologies.

4.2. Fabrication of Polymer Disks. Polymer disks were fabricated by melt-mixing PPC and starch granules. Prior to mixing, the starch granules were visualized with bright field microscopy. The average particle size of these starch granules, calculated by using ImageJ software, was 28.59 ± 2.98 μm. Known amounts of PPC and starch granules were thoroughly melt-mixed at 170 °C for 10 min in a custom-made stainless steel vessel using a stirrer (WiseStir HS30D stirrer) at a rotation speed of 300 rpm. The resulting paste was then placed in a custom-made cylindrical shaped molds; the temperature was slowly decreased to ambient conditions (25 °C) and the sample was stored at room temperature for further characterizations. The produced polymer cylinder was 5 cm in height and 1 cm in diameter, and cut to the desired sizes according to each characterization methods. The composition of starch was varied between 0 and 50 wt % to assess its effect on physicochemical properties of the composites. The resulting PPC−starch composites were denoted as PPC-ST, followed by the weight ratio (percent) of starch. For instance, PPC-ST40 represents the PPC-starch composite with 40 wt % starch and 60 wt % PPC contents.

For in vitro and in vivo animal studies, the samples were prepared in aseptic condition. To confirm the presence of molecular interaction between PPC and starch, attenuated total reflectance-Fourier transform infrared (ATR-FTIR, Varian 660-IR) spectroscopy was used. For each measurement, 32 scans collected with a resolution of 4 cm^{-1} over the range of 1100−1900 cm^{-1}.

4.3. Thermal Analysis. Thermal stability of the composites and PPC was determined by differential scanning calorimetry/thermal gravimetric analysis (DSC/TGA). Measurements were carried out by using a thermal gravimetric analyzer (Mattler Toledo (1/79 Newton Road, Wetherill Park, 2164)) under helium/oxygen (50/50 ratios) gas flow conditions. The weight loss as a function of temperature was measured at a heating rate of 5 °C/min. STAR^e system (version V.9.0×) control software was used for the data analysis. The PPC−starch composite were encapsulated in Al pans and heated with purged dry nitrogen gas flow (50 mL/min). Standard mode DSC measurements were performed at a heating rate of 2 K/min.

DOI: 10.1021/acsami.5b06407
ACS Appl. Mater. Interfaces 2015, 7, 22421−22430

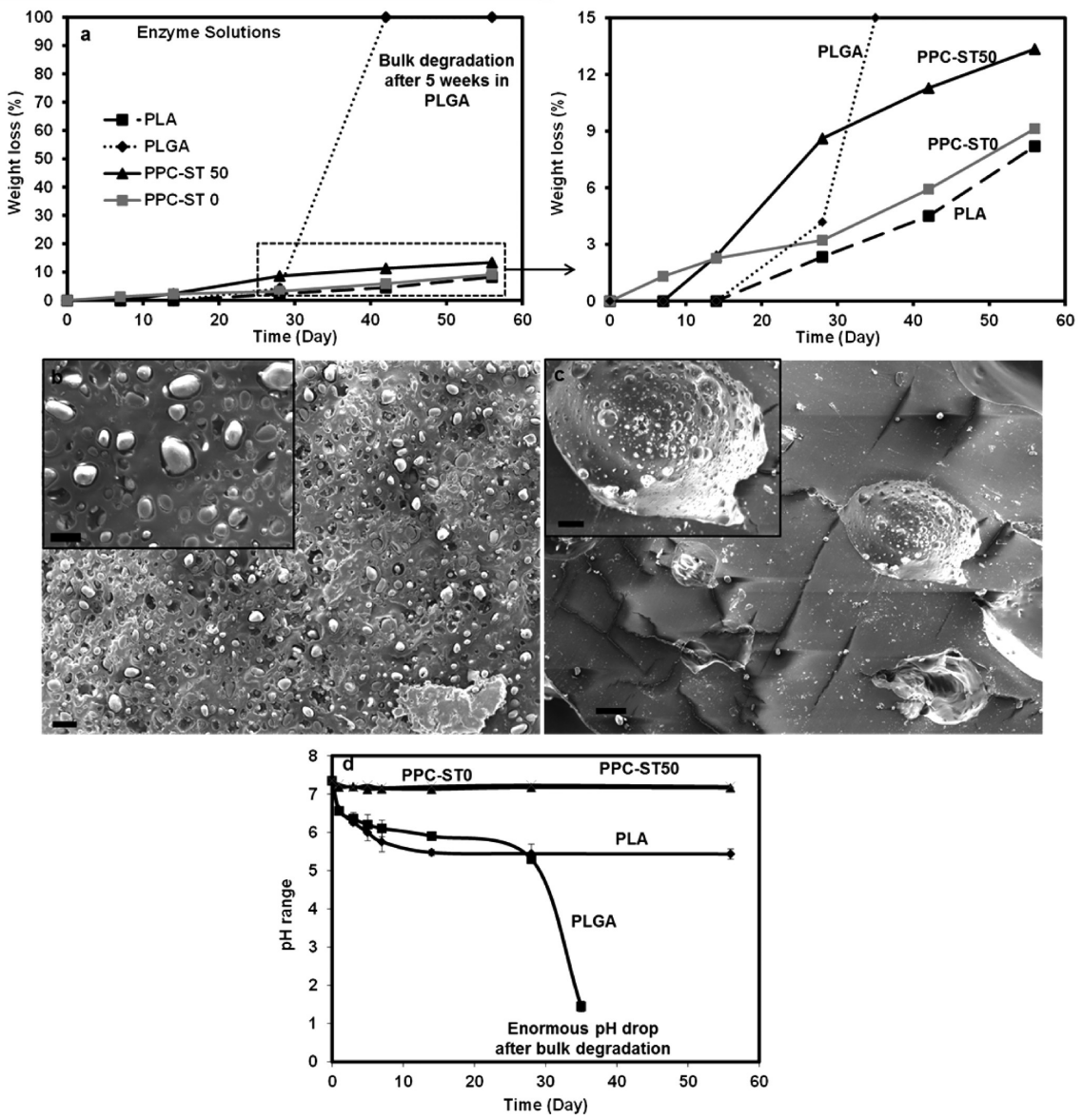

Figure 7. (a) Comparison between the degradation rates of PPC-starch composite with PLA and PLGA in period of two months; SEM images of (b) PPC-ST50, and (c) PPC-ST0 after 8 weeks soaking in enzyme solution, scale bar is 100 μm for large scale models and 50 μm for magnified images; (d) pH values measurements in enzyme solutions for 8 weeks.

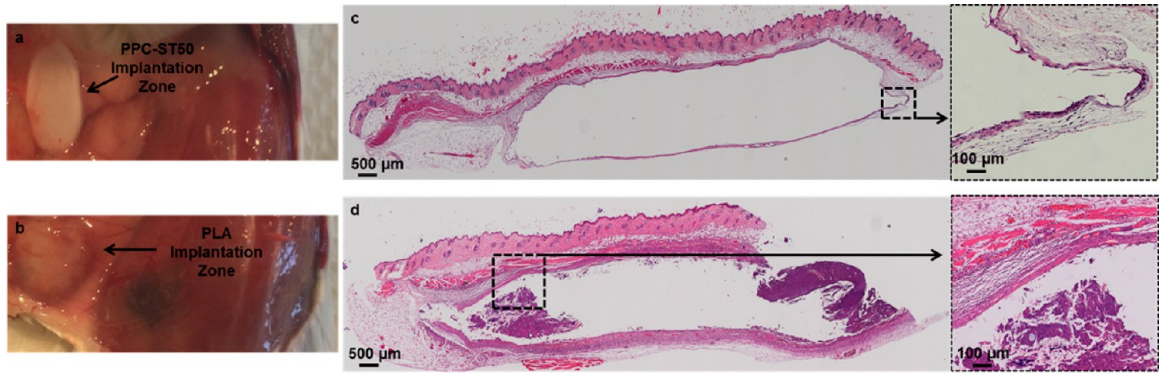

Figure 8. Explanation site of (a) PPC-ST50 and (b) PLA 8 weeks postsurgery, and hematoxylin and eosin staining of paraffin sections of the implantation site at 8 weeks around (c) PPC-ST50 composite and (d) PLA. After 8 weeks a prominent foreign body reaction could be observed in the PLA implantation zone. However, the inflammatory response to the PPC-ST50 composite resolved dramatically. The PPC-ST50 and PLA scaffolds present in the H&E images may not adhere to the glass slides during histological staining.

DOI: 10.1021/acsami.5b06407
ACS Appl. Mater. Interfaces 2015, 7, 22421−22430

4.4. Scanning Electron Microscopy (SEM). Surface morphology and the dispersion of the starch particles within the PPC polymer matrices were examined by Zeiss EVO 50 SEM, operating at an acceleration voltage of 10 kV. The cross-section of samples was mounted on aluminum stubs, using conductive silver paint, and then gold sputtered (Emitech K550X sputter coater) prior to SEM analysis. SEM analysis was also used to examine the cell morphology of the osteoblast cells on the surface of PPC-starch composites within 24 h postculture at different time intervals. For this analysis, the samples were placed in 24 well-plates, and 75 μL of cell suspension was added to each well to have 2×10^5 cells/well. At different time points, the attached cells were fixed in 2.5% glutaraldehyde for 1 h and washed with PBS for at least three times. Polymeric samples incubated at room temperature for another hour in the secondary fixative (1% osmium tetroxide in 0.1 M PBS). Sequential dehydration in various ethanol grades including 30, 50, 70, and 90% and pure ethanol were then performed. The ethanol residues were removed from the samples by using 0.5 mL of hexamethyldisilazane (HMDS) and incubation at room temperature for 2 min. Subsequently, the samples were dried in a desiccator with the lid off to allow the HMDS evaporate overnight. Gold coating was used for the final SEM analysis.

4.5. Mechanical Test. Uniaxial compression tests were performed in an unconfined state by using Instron (model 5543) with a 1000 N load cell using the method describe in the previous study.[53] The compression (mm) and load (N) were obtained at a crosshead speed of 30 μm/s and up to 0.3 mm/mm of strain level. The compressive modulus was then calculated as the tangent slope of stress−strain curves in the linear strain region of 0.1 to 0.2 mm/mm.

4.6. Osteoblast Cell Proliferation. The PPC-ST0 and PPC-ST50 were used for the in vitro cell studies. The aseptic technique was used for the fabrication of these samples. The samples were placed in 24 well-plates, and 50 μL of Saos-2 (Sarcoma osteogenic) cell suspension was added to each well to reach the initial cell count of 2×10^5 per well-plate. Osteoblast cell proliferation was studied by using the MTS assay at different time points, e.g., 1, 3, and 7 days postculture. At each time point, the samples were placed in a new well-plate and rinsed by PBS triple. The washed samples were then soaked in 250 μL of fresh media and 50 μL of MTS solution for 1 h at 37 °C incubator. The viability of cells was quantified by measuring the absorbance of the resulting solutions at 490 nm wavenumbers.

4.7. In Vivo Biocompatibility. The in vivo cytocompatible and the biological properties of the PPC-ST50 and PLA disks were studied by using a mice subcutaneous implantation model. These composites were prefabricated in vitro in an antiseptic condition as described in 4.2. Nine pathogen-free, male BALB/c mice, aged 6 months weighed 28 ± 1.7 g were acquired, housed, and studied under a protocol approved by SLHD Animal Welfare Committee in Sydney, Australia (#2013/019A). Each mouse was anesthetized individually by intraperitoneal injection of a mixture of ketamine (75 mg/mL) and xylazine (10 mg/mL) at 0.01 mL/g of body weight. The dorsal hair was shaved, and the skin was cleaned with betadine solution and washed with sterile saline. The incision was created surgically in the dorsal area and dissected to create a subcutaneous pouch into which the hydrogel was inserted. The wounds were then closed with 5−0 silk sutures and covered by Atrauman (Hartmann, Australia) and IV3000 wound dressings (Smith & Nephew) for 7 days. Carprofen (5 mg/kg) was given at the time of anesthesia and then on the following day postsurgery for analgesia. After surgery, each mouse was caged individually for the first 2 days and then three mice per cage thereafter with free access to water and food. The animal behavior was monitored for signs of pain/distress, restlessness, depression, and lack of appetite. Heart and respiratory rates, body temperature, and their activities were also monitored. The mice maintained their well-being throughout the period of study. Skin biopsies were collected for histological analysis at 1, 2, 4, and 8 weeks postimplantation.

Skin biopsies with implanted conjugated PPC−starch composite were fixed in 100 mg/mL formalin for 24 h. All samples were then dehydrated and embedded in paraffin. The 5 μm sections were deparaffinised in xylene and stained with haematoxylin and eosin (H&E). The samples then mounted on the microscopic slides and were studied by using DM600 Nikon Upright microscope.

4.8. Enzymatic Degradation. Degradation studies were carried out by soaking samples in PBS solution (0.1 M, pH 7.4) containing α-amylase (150 U/L) from *Aspergillus oryzae*, lipase (110 U/L) from *Rhizopus oryzae*, and the coenzyme solution which combined from 110 U/L lipase and 150 U/L α-amylase using PBS as a control. The concentrations of α-amylase and lipase were selected according to the body standard, where serum α-amylase and serum lipase in healthy adults were in the range of 46 to 244U/L and 30 to 190 U/L, respectively.[28] Antibiotic-a (0.2%) was used in all solutions to prevent micro-organism growth. These analyzes were carried out at 37 °C under dynamic conditions using a shaker (BIOLINE-Incubator shaker 4500) at 70 rpm. The surface area of all samples was similar (50 mm^2 and height of 1 mm). At different time points (1 day, 3 days, and 1, 2, 4, 6, and 8 weeks) the washing media was changed to preserve the activity of the enzymes. In addition, at each time point, the pH of solutions was measured, and the gravimetric techniques were used to study the degradation of the composite PPC-starch composites. The weight loss (%) of specimens was calculated by using eq 1, whereas the final weight of samples was obtained after 6 h drying using a vacuum oven at 40 °C.

$$\text{weight loss (\%)} = \left(\frac{\text{initial weight} - \text{final weight}}{\text{initial weight}}\right) \times 100 \quad (1)$$

4.9. Statistical Analysis. Results of mechanical properties, enzymatic degradation, cell toxicity, and cell proliferation were reported as mean ± SDV, acquired from at least three independent experiments at each condition. Statistical analysis ($N = 3$) was performed using a one-way analysis of variance (ANOVA) with a Tukey's multiple comparisons tests for a significance level of $p < 0.05$.

AUTHOR INFORMATION

Corresponding Author

*E-mail: fariba.dehghani@sydney.edu.au. Fax: +612 9351 285. Tel: +612 93514754.

Notes

The authors declare no competing financial interest.

ACKNOWLEDGMENTS

The authors acknowledge the financial support of Australian Research Council and Cardia Bioplastics Ltd. Mr. I.M. also acknowledges the financial support from the Sydney University for the postgraduate scholarship. A.F. acknowledges the financial support from the Australian government for Australian Postgraduate Research Award Scholarship. The authors also acknowledge the facilities and the scientific and technical assistance of the Australian Microscopy & Microanalysis Research Facility at the Electron Microscope Unit, The University of Sydney.

REFERENCES

(1) Middleton, J. C.; Tipton, A. J. Synthetic Biodegradable Polymers as Orthopedic Devices. *Biomaterials* **2000**, *21*, 2335−2346.

(2) Albertsson, A. C.; Varma, I. K. Recent Developments in Ring Opening Polymerization of Lactones for Biomedical Applications. *Biomacromolecules* **2003**, *4*, 1466−1486.

(3) Fambri, L.; Pegoretti, A.; Fenner, R.; Incardona, S. D.; Migliaresi, C. Biodegradable Fibres of Poly(L-Lactic Acid) Produced by Melt Spinning. *Polymer* **1997**, *38*, 79−85.

(4) Wang, Q.; Bao, Y.; Ahire, J.; Chao, Y. Co-Encapsulation of Biodegradable Nanoparticles with Silicon Quantum Dots and Quercetin for Monitored Delivery. *Adv. Healthcare Mater.* **2013**, *2*, 459−66.

DOI: 10.1021/acsami.5b06407
ACS Appl. Mater. Interfaces 2015, 7, 22421−22430

(5) Ding, Z.; Liu, Z.; Wei, W.; Li, Z. Preparation and Characterization of Plla Composite Scaffolds by Scco2-Induced Phase Separation. *Polym. Compos.* **2012**, *33*, 1667−1671.
(6) Danmark, S.; Finne-Wistrand, A.; Schander, K.; Hakkarainen, M.; Arvidson, K.; Mustafa, K.; Albertsson, A. C. Vitro and in Vivo Degradation Profile of Aliphatic Polyesters Subjected to Electron Beam Sterilization. *Acta Biomater.* **2011**, *7*, 2035−2046.
(7) Sui, G.; Yang, X.; Mei, F.; Hu, X.; Chen, G.; Deng, X.; Ryu, S. Poly-L-Lactic Acid/Hydroxyapatite Hybrid Membrane for Bone Tissue Regeneration. *J. Biomed. Mater. Res., Part A* **2007**, *82A*, 445−454.
(8) Doğan, A.; Demirci, S.; Bayir, Y.; Halici, Z.; Karakus, E.; Aydin, A.; Cadirci, E.; Albayrak, A.; Demirci, E.; Karaman, A.; Ayan, A. K.; Gundogdu, C.; Şahin, F. Boron Containing Poly-(Lactide-Co-Glycolide) (Plga) Scaffolds for Bone Tissue Engineering. *Mater. Sci. Eng., C* **2014**, *44*, 246−253.
(9) Chuenjitkuntaworn, B.; Supaphol, P.; Pavasant, P.; Damrongsri, D. Electrospun Poly(L-Lactic Acid)/Hydroxyapatite Composite Fibrous Scaffolds for Bone Tissue Engineering. *Polym. Int.* **2010**, *59*, 227−235.
(10) Zhong, X.; Dehghani, F. Solvent Free Synthesis of Organometallic Catalysts for the Copolymerisation of Carbon Dioxide and Propylene Oxide. *Appl. Catal., B* **2010**, *98*, 101−111.
(11) Zhong, X.; Lu, Z. F.; Valtchev, P.; Wei, H.; Zreiciat, H.; Dehghani, F. Surface Modification of Poly(Propylene Carbonate) by Aminolysis and Layer-by-Layer Assembly for Enhanced Cytocompatibility. *Colloids Surf., B* **2012**, *93*, 75−84.
(12) Wang, Y.; Zhao, Z.; Zhao, B.; Qi, H. X.; Peng, J.; Zhang, L.; Xu, W. J.; Hu, P.; Lu, S. B. Biocompatibility Evaluation of Electrospun Aligned Poly(Propylene Carbonate) Nanofibrous Scaffolds with Peripheral Nerve Tissues and Cells in Vitro. *Chin. Med. J. (Engl.)* **2011**, *124*, 2361−2366.
(13) Nagiah, N.; Sivagnanam, U. T.; Mohan, R.; Srinivasan, N. T.; Sehgal, P. K. Development and Characterization of Electropsun Poly(Propylene Carbonate) Ultrathin Fibers as Tissue Engineering Scaffolds. *Adv. Eng. Mater.* **2012**, *14*, B138−B148.
(14) Luinstra, G. A.; Borchardt, E. Material Properties of Poly-(Propylene Carbonates). *Adv. Polym. Sci.* **2011**, *245*, 29−48.
(15) Liu, H. H.; Pan, L. S.; Lin, Q.; Xu, N.; Lu, L. B.; Pang, S. J.; Fu, S. B. Preparation and Characterization of Poly(Propylene Carbonate)/Polystyrene Composite Films by Melt-Extrusion Method. *e-Polym.*, **2010**, *10*, DOI: 10.1515/epoly.2010.10.1.390.
(16) Du, L. C.; Qu, B. J.; Meng, Y. Z.; Zhu, Q. Structural Characterization and Thermal and Mechanical Properties of Poly-(Propylene Carbonate)/Mgal-Ldh Exfoliation Nanocomposite Via Solution Intercalation Compos. *Compos. Sci. Technol.* **2006**, *66*, 913−918.
(17) Yang, G. H.; Su, J. J.; Gao, J.; Hu, X.; Geng, C. Z.; Fu, Q. Fabrication of Well-Controlled Porous Foams of Graphene Oxide Modified Poly(Propylene-Carbonate) Using Supercritical Carbon Dioxide and Its Potential Tissue Engineering Applications. *J. Supercrit. Fluids* **2013**, *73*, 1−9.
(18) Xie, F. W.; Pollet, E.; Halley, P. J.; Averous, L. Starch-Based Nano-Biocomposites. *Prog. Polym. Sci.* **2013**, *38*, 1590−1628.
(19) Brzeziński, M.; Biela, T. Polylactide Nanocomposites with Functionalized Carbon Nanotubes and Their Stereocomplexes. *Mater. Lett.* **2014**, *121*, 244−250.
(20) Gao, F. Clay/Polymer Composites. *Mater. Today* **2004**, *7*, 50−55.
(21) Hollanda, L. M.; Lobo, A. O.; Lancellotti, M.; Berni, E.; Corat, E. J.; Zanin, H. Graphene and Carbon Nanotube Nanocomposite for Gene Transfection. *Mater. Sci. Eng., C* **2014**, *39*, 288−298.
(22) Obarzanek-Fojt, M.; Elbs-Glatz, Y.; Lizundia, E.; Diener, L.; Sarasua, J.-R.; Bruinink, A. From Implantation to Degradation — Are Poly (L-Lactide)/Multiwall Carbon Nanotube Composite Materials Really Cytocompatible? *Nanomedicine* **2014**, *10*, 1041−1051.
(23) Ghadiri, M.; Chrzanowski, W.; Lee, W. H.; Fathi, A.; Dehghani, F.; Rohanizadeh, R. Physico-Chemical, Mechanical and Cytotoxicity Characterizations of Laponite®/Alginate Nanocomposite. *Appl. Clay Sci.* **2013**, *85*, 64−73.
(24) Rodrigues, A. I.; Gomes, M. E.; Leonor, I. B.; Reis, R. L. Bioactive Starch-Based Scaffolds and Human Adipose Stem Cells Are a Good Combination for Bone Tissue Engineering. *Acta Biomater.* **2012**, *8*, 3765−3776.
(25) Duarte, A. R. C.; Mano, J. F.; Reis, R. L. Preparation of Starch-Based Scaffolds for Tissue Engineering by Supercritical Immersion Precipitation. *J. Supercrit. Fluids* **2009**, *49*, 279−285.
(26) Rodrigues, A.; Emeje, M. Recent Applications of Starch Derivatives in Nanodrug Delivery. *Carbohydr. Polym.* **2012**, *87*, 987−994.
(27) Li, J.; Baker, B. A.; Mou, X.; Ren, N.; Qiu, J.; Boughton, R. I.; Liu, H. Biopolymer/Calcium Phosphate Scaffolds for Bone Tissue Engineering. *Adv. Healthcare Mater.* **2014**, *3*, 469−484.
(28) Martins, A. M.; Pham, Q. P.; Malafaya, P. B.; Sousa, R. A.; Gomes, M. E.; Raphael, R. M.; Kasper, F. K.; Reis, R. L.; Mikos, A. G. The Role of Lipase and Alpha-Amylase in the Degradation of Starch/Poly(Epsilon-Caprolactone) Fiber Meshes and the Osteogenic Differentiation of Cultured Marrow Stromal Cells. *Tissue Eng., Part A* **2009**, *15*, 295−305.
(29) Lu, X. L.; Du, F. G.; Ge, X. C.; Xiao, M.; Meng, Y. Z. Biodegradability and Thermal Stability of Poly(Propylene Carbonate)/Starch Composites. *J. Biomed. Mater. Res., Part A* **2006**, *77A*, 653−658.
(30) Peng, S. W.; Wang, X. Y.; Dong, L. S. Special Interaction between Poly (Propylene Carbonate) and Corn Starch. *Polym. Compos.* **2005**, *26*, 37−41.
(31) Joshi, S. S.; Mebel, A. M. Computational Modeling of Biodegradable Blends of Starch Amylose and Poly-Propylene. *Polymer* **2007**, *48*, 3893−3901.
(32) Ma, X. F.; Yu, H. G.; Zhao, A. Properties of Biodegradable Poly(Propylene Carbonate)/Starch Composites with Succinic Anhydride. *Compos. Sci. Technol.* **2006**, *66*, 2360−2366.
(33) Li, X. H.; Meng, Y. Z.; Chen, G. Q.; Li, R. K. Y. Thermal Properties and Rheological Behavior of Biodegradable Aliphatic Polycarbonate Derived from Carbon Dioxide and Propylene Oxide. *J. Appl. Polym. Sci.* **2004**, *94*, 711−716.
(34) Barreto, C.; Hansen, E.; Fredriksen, S. Novel Solventless Purification of Poly(Propylene Carbonate): Tailoring the Composition and Thermal Properties of Ppc. *Polym. Degrad. Stab.* **2012**, *97*, 893−904.
(35) Gao, Z. W.; Wang, S. F.; Xia, C. G. Synthesis of Propylene Carbonate from Urea and 1,2-Propanediol. *Chin. Chem. Lett.* **2009**, *20*, 131−135.
(36) Abeykoon, C.; Martin, P. J.; Li, K.; Kelly, A. L. Dynamic Modelling of Die Melt Temperature Profile in Polymer Extrusion: Effects of Process Settings. *Screw Geometry and Material Appl. Math. Modell.* **2014**, *38*, 1224−1236.
(37) Zhong, X.; Dehghani, F. Fabrication of Biomimetic Poly-(Propylene Carbonate) Scaffolds by Using Carbon Dioxide as a Solvent. *Green Chem.* **2012**, *14*, 2523−2533.
(38) Antunes, P. V.; Ramalho, A.; Carrilho, E. V. P. Mechanical and Wear Behaviours of Nano and Microfilled Polymeric Composite: Effect of Filler Fraction and Size. *Mater. Eng.* **2014**, *61*, 50−60.
(39) Moulton, S. E.; Wallace, G. G. 3-Dimensional (3d) Fabricated Polymer Based Drug Delivery Systems. *J. Controlled Release* **2014**, *193*, 27−34.
(40) Khaled, S. A.; Burley, J. C.; Alexander, M. R.; Roberts, C. J. Desktop 3d Printing of Controlled Release Pharmaceutical Bilayer Tablets. *Int. J. Pharm.* **2014**, *461*, 105−111.
(41) Goyanes, A.; Buanz, A. B. M.; Basit, A. W.; Gaisford, S. Fused-Filament 3d Printing (3dp) for Fabrication of Tablets. *Int. J. Pharm.* **2014**, *476*, 88−92.
(42) Fathi, A.; Lee, S.; Breen, A.; Shirazi, A. N.; Valtchev, P.; Dehghani, F. Enhancing the Mechanical Properties and Physical Stability of Biomimetic Polymer Hydrogels for Micro-Patterning and Tissue Engineering Applications. *Eur. Polym. J.* **2014**, *59*, 161−170.

DOI: 10.1021/acsami.5b06407
ACS Appl. Mater. Interfaces 2015, 7, 22421−22430

(43) Wang, Q.; Libera, M. Microgel-Modified Surfaces Enhance Short-Term Osteoblast Response. *Colloids Surf., B* **2014**, *118*, 202−9.
(44) Mattila, P. K.; Lappalainen, P. Filopodia: Molecular Architecture and Cellular Functions. *Nat. Rev. Mol. Cell Biol.* **2008**, *9*, 446−54.
(45) Sun, L. G.; Xie, Z. Y.; Zhao, Y. J.; Wei, H. M.; Gu, Z. Z. Optical Monitoring the Degradation of Plga Inverse Opal Film. *Chin. Chem. Lett.* **2013**, *24*, 9−12.
(46) Hoshino, A.; Isono, Y. Degradation of Aliphatic Polyester Films by Commercially Available Lipases with Special Reference to Rapid and Complete Degradation of Poly(L-Lactide) Film by Lipase Pl Derived from Alcaligenes Sp. *Biodegradation* **2002**, *13*, 141−147.
(47) Wan, P.; Yuan, C.; Tan, L.; Li, Q.; Yang, K. Fabrication and Evaluation of Bioresorbable Plla/Magnesium and Plla/Magnesium Fluoride Hybrid Composites for Orthopedic Implants Compos. *Compos. Sci. Technol.* **2014**, *98*, 36−43.
(48) Kon, E.; Roffi, A.; Filardo, G.; Tesei, G.; Marcacci, M. Scaffold-Based Cartilage Treatments: With or without Cells? *A Systematic Review of Preclinical and Clinical Evidence Arthroscopy* **2015**, *31*, 767−775.
(49) Filardo, G.; Kon, E.; Roffi, A.; Di Martino, A.; Marcacci, M. Scaffold-Based Repair for Cartilage Healing. *A Systematic Review and Technical Note Arthroscopy* **2013**, *29*, 174−186.
(50) Hou, P.; Troen, T.; Ovejero, M. C.; Kirkegaard, T.; Andersen, T. L.; Byrjalsen, I.; Ferreras, M.; Sato, T.; Shapiro, S. D.; Foged, N. T.; Delaissé, J.-M. Matrix Metalloproteinase-12 (Mmp-12) in Osteoclasts. *New Lesson on the Involvement of Mmps in Bone Resorption Bone* **2004**, *34*, 37−47.
(51) Zhou, H.; Lawrence, J. G.; Bhaduri, S. B. Fabrication Aspects of Pla-Cap/Plga-Cap Composites for Orthopedic Applications. *Acta Biomater.* **2012**, *8*, 1999−2016.
(52) Grayson, A. C. R.; Voskerician, G.; Lynn, A.; Anderson, J. M.; Cima, M. J.; Langer, R. Differential Degradation Rates in Vivo and in Vitro of Biocompatible Poly(Lactic Acid) and Poly(Glycolic Acid) Homo- and Co-Polymers for a Polymeric Drug-Delivery Microchip. *J. Biomater. Sci., Polym. Ed.* **2004**, *15*, 1281−1304.
(53) Fathi, A.; Mithieux, S. M.; Wei, H.; Chrzanowski, W.; Valtchev, P.; Weiss, A. S.; Dehghani, F. Elastin Based Cell-Laden Injectable Hydrogels with Tunable Gelation. *Biomaterials* **2014**, *35*, 5425−5435.

DOI: 10.1021/acsami.5b06407
ACS Appl. Mater. Interfaces 2015, 7, 22421−22430